Published in final edited form as:
J Neurosci Res. 2009 February 15; 87(3): 668–676. doi:10.1002/jnr.21877.

Ultrastructural and Temporal Changes of the Microvascular Basement Membrane and Astrocyte Interface Following Focal Cerebral Ischemia

Il Kwon[1], **Eun Hee Kim**[1], **Gregory J. del Zoppo**[2], and **Ji Hoe Heo**[1,*]

[1]Department of Neurology, National Core Research Center for Nanomedical Technology, Yonsei University College of Medicine, Seoul, Korea

[2]Departments of Medicine and Neurology, University of Washington, Seattle, Washington

Abstract

Microvascular integrity is lost during cerebral ischemia. Detachment of the microvascular basement membrane (BM) from the astrocyte, as well as degradation of the BM, is responsible for the loss of microvascular integrity. However, their ultrastructural and temporal changes during cerebral ischemia are not well known. Male Sprague-Dawley rats were subjected to permanent middle cerebral artery occlusion (MCAO) for 1, 4, 8, 12, 16, 20, and 48 hr. By using transmission electron microscopy, the proportion of intact BM–astrocyte contacts and electron densities of the BM were measured from five randomly selected microvessels in the ischemic basal ganglia. Their temporal changes and associations with activities of the matrix metalloproteinases (MMPs) were investigated. The intact portion of the BM–astrocyte contacts was decreased significantly within 4 hr and was rarely observed at 48 hr after MCAO. Decreases in the electron density and degradation of the BM were significant 12 hr after MCAO. The intact BM–astrocyte contacts and the mean BM density showed a significant positive correlation ($r = 0.784$, $P < 0.001$). MMP-9 activity was correlated negatively with the intact BM–astrocyte contacts ($r = -0.711$, $P < 0.001$) and with the BM density ($r = -0.538$, P 5 0.0016). The increase in MMP-9 coincided temporally with the loss of the BM–astrocyte contacts and a decrease in the BM density. Ultrastructural alterations occurring in the microvascular BM and its contacts with astrocyte endfeet were temporally associated in cerebral ischemia. Time courses of their alterations should be considered in the treatment targeted to the microvascular BM and its contact with astrocytes.

Keywords

cerebral ischemia; astrocytes; basement membrane; electron microscopy

Brain edema and hemorrhagic transformation are major consequences of cerebral ischemic injury. Brain edema is the leading cause of death during the first week after cerebral infarction (Vahedi et al., 2007), and hemorrhagic transformation is a major obstacle of thrombolytic treatment, diminishing its efficacy. Both pathologic conditions are associated with damage to the cerebral microvessels. In addition, microvascular damage may contribute to cell death (Heo et al., 1999). In this regard, protection of the microvessels from ischemic injury could be a major target for specific treatments in acute stroke patients.

*Correspondence to: Ji Hoe Heo, MD, PhD, Department of Neurology, Yonsei University College of Medicine, 250 Seongsanno, Seodaemoongu, 120–752 Seoul, Korea. E-mail: E-mail: jhheo@yuhs.ac.

The cerebral microvessels are a constituent of the blood–brain barrier (BBB), which is composed of microvascular endothelial cells, the basement membrane (BM), astrocyte endfeet, and pericytes (Ballabh et al., 2004). The BM attaches endothelial cells to one side and astrocyte endfeet to the other side. The astrocyte endfeet form an envelope around the blood vessels and are attached to the BM tightly by their adhesion molecules. The BM is composed of extracellular matrix (ECM) molecules such as type IV collagen, laminins, fibronectin, heparan sulfates, and proteoglycans. The integrity of the microvessels is maintained by the presence of an intact BM that provides structural support to the endothelial cell wall and astrocytes. The intact BM is also critical in delivering communicative signals between the intravascular components and the glial/neuronal cells and in providing cellular nutritional support from the blood (Iadecola, 2004; Jan et al., 2004; del Zoppo and Milner, 2006).

Loss of microvascular integrity induced by cerebral ischemia has been demonstrated in pioneering studies in nonhuman primates, which showed a decrease in the ECM molecules and integrins that attach the BM to the endothelium and astrocyte endfeet in the ischemic area (Hamann et al., 1995; Wagner et al., 1997). Over the last decade, several studies have shown that degradation of the microvascular BM is mediated by the uncontrolled activity of proteases (Rosenberg et al., 1996; Heo et al., 1999; Chang et al., 2003; Fukuda et al., 2004). Among the proteases, matrix metalloproteinases (MMPs), particularly MMP-9 and MMP-2, are key enzymes in degrading the ECM components of the BM, and their increases are known to be associated with brain edema, hemorrhagic transformation, and ischemic injury after cerebral ischemia (Rosenberg et al., 1998; Heo et al., 1999, 2003, 2005; Rosell et al., 2006; Zhao et al., 2007).

Molecular pathways involved in the degradation of the microvascular BM may be suitable targets for the specific treatment of brain edema, hemorrhagic transformation, and possibly anoikis-type cell death in stroke patients. These treatments should be initiated before the damage is serious or irreversible. However, temporal patterns of microvascular damage such as detachment of the BM–astrocyte contact and degradation of the BM are not well known. In this study, the temporal changes in the cerebral microvascular BM and surrounding astrocyte contacts and the density of the BM were examined with transmission electron microscopy (TEM) in rats subjected to permanent middle cerebral artery occlusion (MCAO). Additionally, their temporal relationships with MMP activities were investigated.

MATERIALS AND METHODS

Experimental Animals and Preparation

Male Sprague-Dawley (SD) rats weighing 250–320 g were used. The care and use of laboratory animals in this experiment were performed according to the institutionally approved protocol in accordance with the National Institutes of Health's *Guide for the care and use of laboratory animals.* For operative procedures, the animals were anesthetized with an inhalation of 5% isofluorane in a mixture of 70% N_2O and 30% O_2. Anesthesia was maintained with 2% isofluorane. During the operative procedures, body temperature was monitored continuously with a rectal probe and was maintained at 37.0°C ± 0.5°C by means of a homeothermic blanket control unit and heating pad (Harvard Apparatus, Holliston, MA). The left femoral artery was cannulated with PE-50 tubing for the monitoring of arterial blood pressure with a pressure transducer (Harvard Apparatus) and for the analysis of arterial pH, PaO_2, $PaCO_2$, and hemoglobin concentration before and after MCAO (OPTI critical care analyze; AVL Scientific Corporation, Roswell, GA). Regional cerebral blood flow (rCBF) was determined in the territory of the MCA (1 mm caudal to the bregma and 3 mm lateral to the midline) by laser-Doppler flowmetry (LDF; BLF 21 laser Doppler flowmeter; Transonic Systems Inc., Ithaca, NY).

Induction of Acute Focal Cerebral Ischemia and Experimental Groups

The rats were subjected to permanent MCAO, as described previously (Choi et al., 2007), for 1, 4, 8, 12, 16, 20, and 48 hr (five in each group). Four rats were used for controls and underwent the sham operation, which was performed in the same manner as MCAO, except that the MCA was not occluded.

Motor Disability Test

Neurologic evaluation was performed before and after MCAO and before sacrifice. All surviving animals were graded on a known scale (Garcia et al., 1995). Briefly, six items were evaluated. Zero to three points were given to each item when an animal had a deficit and summed for a total score. The minimum neurologic score is 3 and the maximum is 18. The items evaluated were 1) ability to approach all four walls of the cage, 2) symmetry in the movement of four limbs, 3) forepaw outstretching, 4) climbing and gripping abilities on the wire cage, 5) reaction to stimulus on both sides of body, and 6) response to vibrissae touch.

Brain Tissue Preparation

All animals were sacrificed by transcardiac perfusion with cold heparinized normal saline using a peristaltic pump under deep anesthesia with an intraperitoneal urethane injection. The removed brains were sectioned into 2-mm-thick coronal blocks using a rat brain matrix. The fourth coronal blocks from the frontal pole were prefixed with a Karnovsky solution (2% glutaraldehyde, 2% paraformaldehyde, 0.5% $CaCl_2$) and used for TEM.

The third blocks of the brain were divided into ischemic and nonischemic hemispheres. The divided blocks were embedded into cryomolds with Tissue-Tek OCT compound (Miles Inc., Elkahart, IN) and quick-frozen with 2-methylbutan, cooled with dry ice, and then stored at −80°C. These frozen blocks were used for gelatin zymography.

Extraction of Protein and Purification of MMPs

The 50 cryostat 10 μm-thick frozen sections were homogenized with 400 μl of working buffer (50 mM Tris HCl, pH 7.5, 150 ml NaCl, 5 mM $CaCl_2$, 0.05% BRIJ-35, 0.02% NaN_3, 1% Triton X-100) containing 1 mM phenylmethylsulfonyl fluoride and centrifuged at 4°C and 9,000 rpm for 20 min. MMPs were purified based on a method using gelatin-sepharose 4B (Choi et al., 2007). Briefly, after rinsing 50 μl of gelatin-sepharose 4B (Pharmacia Biotech, Uppsala, Sweden) with 200 μl of working buffer three times, the protein extracts were mixed and incubated on a rocking plate for 30 min at 4°C. Then, the samples were centrifuged at 7,000 rpm for 5 min, rinsed with 200 μl working buffer, and centrifuged again. The precipitates were added to 50 μl of elution buffer (working buffer to which 10% dimethylsulfoxide had been added) and incubated for 30 min, while rocking at 4°C. After centrifugation, the supernatant was taken and stored at −80°C until needed for gelatin zymography.

Gelatin Zymography

The purified protein extracts were mixed with an equal volume of sample buffer [80 mM Tris-HCl, pH 6.8, 4% sodium dodecyl sulfate (SDS), 10% glycerol, 0.01% bromophenol blue] and were subjected to zymography as previously published (Heo et al., 1999; Choi et al., 2007). The gelatinolytic activity of these samples was detected by 8% SDS-polyacrylamide gel containing 1% gelatin. Sample gels were rinsed in 150 ml of 2.5% Triton X-100 (15 min) and incubated with 250 ml of 50 mmol/liter Tris-HCl buffer (pH 7.5, 10 mM $CaCl_2$, 0.02% NaN_3) for 43 hr at 37°C. After incubation, the gels were stained with 0.1% amido black containing acetic acid, methanol, and distilled water (volume ratio 1:3:6) for 1 hr and then destained by four washes with the same solution without amido black for 130 min. These gels

were scanned using a flatbed scanner, and the gelatinolytic bands were analyzed and quantified by means of a gel plotting macro using the Scion Image program.

Transmission Electron Microscopy

For electron microscopic observations, the fourth blocks of the brain were fixed with glutaraldehyde in 2% paraformaldehyde overnight at 4°C, washed in 0.1 M phosphate buffer, pH 7.4, and then postfixed in 1% osmium tetroxide in the same buffer for 15 min. Then, the specimens were dehydrated through a graded series of ethanol, exchanged through propylene oxide, and embedded in a mixture of Epon. Subsequently, ultrathin sections were obtained by ultramicrotome (Ultracut UCT; Leica, Australia) with a diamond knife. The sections (1 mm × 1 mm) were obtained from ischemic core area of the basal ganglia of each animal (Fig. 1), where an infarction is consistently found in this model. The presence of ischemic injury in each animal was ensured by occurrence of neurologic deficits. Ultrathin sections were doubly stained with uranyl acetate and lead citrate and examined in a TEM (JEOL-1011; JEOL, Tokyo, Japan) at 80 kV.

Measurements of the Microvascular BM–Astrocyte Contacts and of the Mean BM Density

The proportion of intact BM–astrocyte contacts and the mean electron density of the BM were measured from five randomly selected microvessels in the ischemic basal ganglia by using Scion Image. The circumferential length of the microvessel and the length of the intact astrocyte endfeet that attaches to the BM were measured. The percentage of the intact contact (the length of intact BM–astrocyte contact/total circumferential length of the microvessel × 100) was calculated (Fig. 2). The mean density of the BM was expressed as pixel values ranging from 0 to 255. The value was normalized to that of the darkest regions of the adjacent three myelin sheaths, because the densities of the myelin sheaths were not different among the subjects measured (238.27 ± 15.21, $P = 0.151$). All measurements were performed by a researcher blinded to the sample origins and groups.

Statistical Analysis

All of the statistical computations were performed with SAS version 8.2 (SAS Institute, Cary, NC). The differences among all of the groups were compared by a Kruskal-Wallis test, followed by a post hoc Dunn's method (MMP activities and neurological deficits). The proportion of BM–astrocyte contacts and the density of the BM and myelin sheaths were compared by a one-way ANOVA test, followed by post hoc Duncan's method. Differences in physiological variables and rCBF were compared by means of a paired *t*-test. Correlations among the BM–astrocyte contact, BM density, and MMP-9 activity were evaluated by using a Spearman's test. The values are presented as a mean ± SD. $P < 0.05$ was considered significant.

RESULTS

Mortality and Neurological Outcome

Two of the thirty-five rats (5.7%) that underwent MCAO died, and all four rats that underwent the sham operation survived. After excluding five rats that did not have any neurologic deficits after MCAO, 28 rats were finally included in this study [MCAO for 1 hr (n = 4), 4 hr (n = 5), 8 hr (n = 4), 12 hr (n = 4), 16 hr (n = 4), 20 hr (n = 4), and 48 hr (n = 3)]. The mean scores of neurologic deficits were 8.79 ± 1.55, and the scores among the groups were not different from one another.

No significant changes were noted in the mean arterial blood pressure, pH, $PaCO_2$, PaO_2, or hemoglobin before or after the MCAO. The mean rCBF was decreased by about 74.4% of the baseline 30 min after MCAO.

Temporal Changes in the Neurovascular Unit

Microvascular BM–astrocyte contacts—In sham-operated rats, 94.08% ± 6.04% of the microvascular surface was covered by astrocyte endfeet. At 1 hr after MCAO, the area of the microvascular BM that was ensheathed by the astrocyte endfeet was reduced to 85.74% ± 9.45% (Fig. 3). The reduction of the intact areas of the BM–astrocyte contacts was significant at 4 hr after MCAO (74.08% ± 7.83%, $P < 0.05$) and thereafter in a time-dependent manner. At 16 hr, the loss of the BM–astrocyte contacts was marked, in that only 15.92% ± 17.54% of the BM was attached to the astrocyte endfeet, and the contacts were rarely observed 48 hr after MCAO.

Electron density changes in the microvascular BM—Changes in the BM were assessed by measuring its electron density and morphology (Fig. 4). The BM appeared homogenously dark and compact, and its margin was clean in the sham-operated rats. In ischemic rats, the mean values of the electron corrected BM density were decreased in a time-dependent manner. From 12 hr after MCAO, destruction of the BM was evident in that its margin appeared fuzzy and the decrease in its density was significant (Fig. 4E). At 48 hr after MCAO, the BM was very faint and sparse, and the mean density was decreased to 69% that of the sham-operated rats (Fig. 4H).

Astrocytes and surrounding tissues—In the sham-operated rats, the cellular components and adjacent matrix were undamaged and compact (Fig. 4A). Mildly swollen astrocyte endfeet began to be seen occasionally in the ischemic core region 1 hr after MCAO (Fig. 4B). At 8 hr, the electron micrograph depicts seriously swollen and pale astrocyte endfeet abutting a microvessel with noticeable tissue damage (Fig. 4D). At 16 hr after MCAO, damage to the surrounding brain tissue as well as the BM was severe. Extravasation of water caused by the rupture of a swollen astrocytic plasma membrane and/or disruption of the BBB was evident (Fig. 4F). Accumulated fluid was not localized to the pericapillary space but was found to be scattered throughout the surrounding tissues at 48 hr after ischemia.

MMP Activity

MMP-9 activity was detected at 1 hr after MCAO in the ischemic hemisphere and increased at 4 hr. The increase was significant at 12 hr after MCAO. However, MMP-2 activity was not increased in either ischemic or nonischemic hemispheres at any time points examined until 48 hr after MCAO (Fig. 5).

Pattern of Changes in the Neurovascular Unit and MMP-9 Activity

The gross pattern of temporal changes in the loss of BM–astrocyte contacts and the decrease of BM density appeared parallel (Fig. 3A). However, the focal loss of contacts was evident very early after MCAO and seemed to occur before the rise of MMP-9 (Fig. 3B) or decrease of the BM density (Fig. 3A). The loss of BM–astrocyte contacts and increase of MMP-9 seemed to be parallel in a time-dependent manner from 4 hr to 12 hr after MCAO. Despite the fact that the increase of MMP-9 ceased after 16 hr, the loss of contacts continued for 48 hr (Fig. 3B).

Correlation Among Loss of the BM–Astrocyte Contacts, BM Density, and MMP-9 Activity

The relationship between an increase in a matrix-degrading protease (MMP-9) and damage to the BM (BM density and BM–astrocyte contacts) in each animal was also assessed (Fig. 6). The intact BM–astrocyte contacts and the mean BM density showed a strong association ($r = 0.784$, $P < 0.0001$; Fig. 6A). The mean BM density and the MMP-9 activity exhibited a negative correlation ($r = -0.538$, $P = 0.0016$; Fig. 6B). There was a strong negative correlation between the proportion of the intact BM–astrocyte contacts and the MMP-9 activity ($r = -0.711$, $P < 0.0001$; Fig. 6C).

DISCUSSION

Cerebral ischemia affects not only glial and neuronal cells but also microvessels. Thus, the functional concept of the neurovascular unit, which emphasizes structural and functional linkages among microvessels, astrocytes, and neurons, constitutes an important understanding of the ischemic injury mechanism as well as the normal physiology of the brain (Lo et al., 2003). Previous studies provided evidence of a loss of microvascular integrity after cerebral ischemia in the form of a decrease in immunoreactivity to the vascular ECM molecules of the vascular BM, loss of matrix adhesion receptors that attach the BM to astrocyte endfeet, increase of proteinases that degrade vessel wall ECM components, and preservation of the BBB-associated proteins by an MMP-9 gene knockout (Heo et al., 1999; Asahi et al., 2000; Fukuda et al., 2004). The present study shows evidence of damage occurring in the BM and its adhering contacts to astrocytes in a straightforward manner by demonstrating changes in the ultrastructural morphology.

The electron microscopic appearance of a sparse BM and a decrease in the electron density of the BM in this study may represent degradation and a resultant decrease of the microvascular ECM molecules in the ischemic core. In nonhuman primates and mice, antigen losses for type IV collagen, fibronectin, and laminin were approximately 55–75% of the control subjects after 24 hr of reperfusion following 3 hr of MCAO (Hamann et al., 1995; Vosko et al., 2003). In the present study, the electron density of the BM was decreased to 71% at 20 hr and 69% at 48 hr of MCAO, which was very similar to that observed in nonhuman primates and mice based on the immunohistochemical detection of ECM molecules. The significant decrease in electron density appeared after a longer ischemic time (12 hr of MCAO) in this study, which is consistent with the observations in previous studies (Vosko et al., 2003). After this time point, fluid was seen in the extracellular and extravascular space. Vasogenic edema, which is caused by uncontrolled fluid leakage from the blood to the brain parenchyma through a damaged BBB, contributes to an actual net volume increase of the brain (Heo et al., 2005). Brain swelling usually reaches its maximum 2–5 days after cerebral infarction. However, the temporal patterns of BM degradation in our study suggest that therapeutic strategies aimed at reducing brain edema based on targeting specific molecular pathways involved in BM degradation should be initiated as soon as possible and start before the BM suffers significant damage (at least 12 hr after onset).

It has been postulated that degradation of the microvascular BM and BBB damage results from an increased MMP (Asahi et al., 2001). MMP-9 is known to be maximally increased at 12–24 hr, whereas MMP-2 increases during a later time period after cerebral ischemia in rats (Rosenberg et al., 1996; Heo et al., 2005), consistently with findings in this study. In an ex vivo assay, microvascular ECM molecules of normal brain tissues were degraded when supernatants from ischemic brain tissues were applied to them, which was inhibitable by MMP inhibitors. This indicates that MMPs generated in the ischemic brain play a role in BM degradation (Fukuda et al., 2004). The present study adds further evidence by demonstrating that there were inverse relationships between the MMP-9 activity and both BM density and BM–astrocyte contacts and that the degradation of the BM was strongly correlated with the loss of BM–astrocyte contacts. These findings suggest that an increased MMP-9 activity contributed to the degradation of ECM molecules and resultant disruption of the normal attachment of the BM to astrocyte endfeet.

In this study, temporal changes occurring in the BM and MMP-9 activities coincided. The increase in MMP-9, decrease in BM density, and loss of BM–astrocyte contacts paralleled each other from 4 hr to 12 hr after MCAO. After this time, damage to the BM was more extensive, and further loss of the contacts was seen. Most MMP-9 activities that were detected on zymographic studies were latent forms. To degrade ECM molecules, latent MMP-9, after its

secretion, should be activated by a proteolytic deletion of the propeptide region. The enzymatic activity of MMPs on zymographic gels increases with longer incubation times (Kleiner and Stetlerstevenson, 1994). Therefore, continuing degradation of the BM after a maximal increase of MMP-9 activity in this study may be explainable.

Notably, the loss of the BM–astrocyte contacts appeared before the increase of MMP-9 or decrease of BM density. Loss of the BM–astrocyte contacts occurred within 4 hr after ischemia, which suggests that the loss of microvascular integrity develops very early after ischemia. Matrix-degrading proteases other than MMPs may contribute to the loss of microvascular integrity in cerebral ischemia. Cysteine proteases, including cathepsins B and L, are suggested to contribute to the loss of perlecan, a component of heparan sulfate proteoglycan in the vascular matrix. The loss of perlecan occurred 1 hr after cerebral ischemia, which was much faster than the loss of laminin, collagen type IV, or fibronectin (Fukuda et al., 2004). In addition to the degradation of the microvascular BM, the loss of vascular adhesion receptors that normally glue the microvascular BM to the astrocytes may play a role in the detachment. Loss of immunoreactivity to integrin $\alpha_6\beta_4$ was observed within 1–2 hr (Wagner et al., 1997) and that of the endothelial cell β_1-integrin expression by 2 hr after MCAO in the ischemic core (Tagaya et al., 2001). Dystroglycan, which forms a physical link between the intracellular cytoskeleton and the vascular ECM, may be involved in early detachment (del Zoppo and Milner, 2006). In view of the facts that the decrease of the integrins occurs very early after ischemia and that the destruction of the BM was seen relatively late in this study, the loss of matrix adhesion receptors may contribute to the early focal detachment of the contacts.

Alterations in the microvascular BM and its interface with astrocytes were coupled with those in the surrounding tissues and astrocytic processes. Swelling of the astrocytes occurs within 5 min of an energy crisis (Dodson et al., 1977). The aquaporin-4, which is a water channel protein and mediates astrocyte swelling, increased in the astrocyte endfeet 1 hr after cerebral ischemia (Ribeiro Mde et al., 2006). Mild astrocytic swelling appeared as early as 1 hr after MCAO in this study, which matches well the time course of aquaporin-4. After 4 hr of ischemia, severe swelling and decreased density of the astrocytic processes were observed. Astrocytes that were swollen and detached from the microvascular BM resulted in rupture of their membranes, which highlights the importance of cell–ECM contact for cell survival. An extravascular collection of fluid was first seen when the BM damage was significant and was confined around the microvessels. However, at the time when the microvascular BM was more severely damaged and the astrocyte endfeet were no longer visible, the extravasated fluid was scattered throughout the brain.

The present study has shown that ultrastructural alterations occurring in the microvascular BM, BM–astrocyte contacts, and matrix degrading MMP-9 during cerebral ischemia have close relationships. Knowledge of the temporally coordinated pattern of the changes in cerebral ischemia, which was investigated in this study, can elucidate the pathological processes that occur dynamically in the neurovascular unit. This may help to initiate a protocol for the appropriate timing of interventional therapies targeted for the protection of the microvascular BM and astrocyte interface. However, this study was conducted in the rat model with permanent MCAO. Although it is possible that temporal changes occurring in the BM and astrocyte interface may be different between permanent and transient ischemic models, temporal changes following transient MCAO were not investigated in our experiment. Therefore, this point should be considered in interpretation of our data.

Acknowledgments

Contract grant sponsor: Korea Research Foundation Grant funded by the Korean Government (MOEHRD); Contract grant sponsor: Basic Research Promotion Fund; Contract grant number: KRF-2007-313-E00406.

REFERENCES

Asahi M, Asahi K, Jung JC, del Zoppo GJ, Fini ME, Lo EH. Role for matrix metalloproteinase 9 after focal cerebral ischemia: effects of gene knockout and enzyme inhibition with BB-94. J Cereb Blood Flow Metab 2000;20:1681–1689. [PubMed: 11129784]

Asahi M, Wang X, Mori T, Sumii T, Jung JC, Moskowitz MA, Fini ME, Lo EH. Effects of matrix metalloproteinase-9 gene knockout on the proteolysis of blood–brain barrier and white matter components after cerebral ischemia. J Neurosci 2001;21:7724–7732. [PubMed: 11567062]

Ballabh P, Braun A, Nedergaard M. The blood–brain barrier: an overview: structure, regulation, and clinical implications. Neurobiol Dis 2004;16:1–13. [PubMed: 15207256]

Chang DI, Hosomi N, Lucero J, Heo JH, Abumiya T, Mazar AP, del Zoppo GJ. Activation systems for latent matrix metalloproteinase-2 are upregulated immediately after focal cerebral ischemia. J Cereb Blood Flow Metab 2003;23:1408–1419. [PubMed: 14663336]

Choi SA, Kim EH, Lee JY, Nam HS, Kim SH, Kim GW, Lee BI, Heo JH. Preconditioning with chronic cerebral hypoperfusion reduces a focal cerebral ischemic injury and increases apurinic/apyrimidinic endonuclease/redox factor-1 and matrix metalloproteinase-2 expression. Curr Neurovasc Res 2007;4:89–97. [PubMed: 17504207]

del Zoppo GJ, Milner R. Integrin-matrix interactions in the cerebral microvasculature. Arterioscler Thromb Vasc Biol 2006;26:1966–1975. [PubMed: 16778120]

Dodson RF, Chu LW, Welch KM, Achar VS. Acute tissue response to cerebral ischemia in the gerbil. An ultrastructural study. J Neurol Sci 1977;33:161–170. [PubMed: 903780]

Fukuda S, Fini CA, Mabuchi T, Koziol JA, Eggleston LL Jr, del Zoppo GJ. Focal cerebral ischemia induces active proteases that degrade microvascular matrix. Stroke 2004;35:998–1004. [PubMed: 15001799]

Garcia JH, Wagner S, Liu KF, Hu XJ. Neurological deficit and extent of neuronal necrosis attributable to middle cerebral artery occlusion in rats. Statistical validation. Stroke 1995;26:627–634. [PubMed: 7709410]discussion 635.

Hamann GF, Okada Y, Fitridge R, del Zoppo GJ. Microvascular basal lamina antigens disappear during cerebral ischemia and reperfusion. Stroke 1995;26:2120–2126. [PubMed: 7482660]

Heo JH, Lucero J, Abumiya T, Koziol JA, Copeland BR, del Zoppo GJ. Matrix metalloproteinases increase very early during experimental focal cerebral ischemia. J Cereb Blood Flow Metab 1999;19:624–633. [PubMed: 10366192]

Heo JH, Kim SH, Lee KY, Kim EH, Chu CK, Nam JM. Increase in plasma matrix metalloproteinase-9 in acute stroke patients with thrombolysis failure. Stroke 2003;34:e48–e50. [PubMed: 12750540]

Heo JH, Han SW, Lee SK. Free radicals as triggers of brain edema formation after stroke. Free Radic Biol Med 2005;39:51–70. [PubMed: 15925278]

Iadecola C. Neurovascular regulation in the normal brain and in Alzheimer's disease. Nat Rev Neurosci 2004;5:347–360. [PubMed: 15100718]

Jan Y, Matter M, Pai J-T, Chen Y-L, Pilch J, Komatsu M, Ong E, Fukuda M, Ruoslahti E. A mitochondrial protein, Bit1, mediates apoptosis regulated by integrins and Groucho/TLE corepressors. Cell 2004;116:751–762. [PubMed: 15006356]

Kleiner DE, Stetlerstevenson WG. Quantitative zymography: detection of picogram quantities of gelatinases. Anal Biochem 1994;218:325–329. [PubMed: 8074288]

Lo EH, Dalkara T, Moskowitz MA. Mechanisms, challenges and opportunities in stroke. Nat Rev Neurosci 2003;4:399–414. [PubMed: 12728267]

Ribeiro Mde C, Hirt L, Bogousslavsky J, Regli L, Badaut J. Time course of aquaporin expression after transient focal cerebral ischemia in mice. J Neurosci Res 2006;83:1231–1240. [PubMed: 16511868]

Rosell A, Ortega-Aznar A, Alvarez-Sabin J, Fernandez-Cadenas I, Ribo M, Molina CA, Lo EH, Montaner J. Increased brain expression of matrix metalloproteinase-9 after ischemic and hemorrhagic human stroke. Stroke 2006;37:1399–1406. [PubMed: 16690896]

Rosenberg GA, Navratil M, Barone F, Feuerstein G. Proteolytic cascade enzymes increase in focal cerebral ischemia in rat. J Cereb Blood Flow Metab 1996;16:360–366. [PubMed: 8621740]

Rosenberg GA, Estrada EY, Dencoff JE, Hsu CY. Matrix metalloproteinases and TIMPs are associated with blood–brain barrier opening after reperfusion in rat brain. Editorial comment. Stroke 1998;29:2189–2195. [PubMed: 9756602]

Tagaya M, Haring HP, Stuiver I, Wagner S, Abumiya T, Lucero J, Lee P, Copeland BR, Seiffert D, del Zoppo GJ. Rapid loss of microvascular integrin expression during focal brain ischemia reflects neuron injury. J Cereb Blood Flow Metab 2001;21:835–846. [PubMed: 11435796]

Vahedi K, Hofmeijer J, Juettler E, Vicaut E, George B, Algra A, Amelink GJ, Schmiedeck P, Schwab S, Rothwell PM, Bousser MG, van der Worp HB, Hacke W. Early decompressive surgery in malignant infarction of the middle cerebral artery: a pooled analysis of three randomised controlled trials. Lancet Neurol 2007;6:215–222. [PubMed: 17303527]

Vosko MR, Busch E, Burggraf D, Bultemeier G, Hamann GF. Microvascular basal lamina damage in thromboembolic stroke in a rat model. Neuroscience Letters 2003;353:217–220. [PubMed: 14665420]

Wagner S, Tagaya M, Koziol JA, Quaranta V, del Zoppo GJ. Rapid disruption of an astrocyte interaction with the extracellular matrix mediated by integrin α6 during focal cerebral ischemia/reperfusion. Stroke 1997;28:858–865. [PubMed: 9099208]

Zhao B-Q, Tejima E, Lo EH. Neurovascular proteases in brain injury, hemorrhage and remodeling after stroke. Stroke 2007;38:748–752. [PubMed: 17261731]

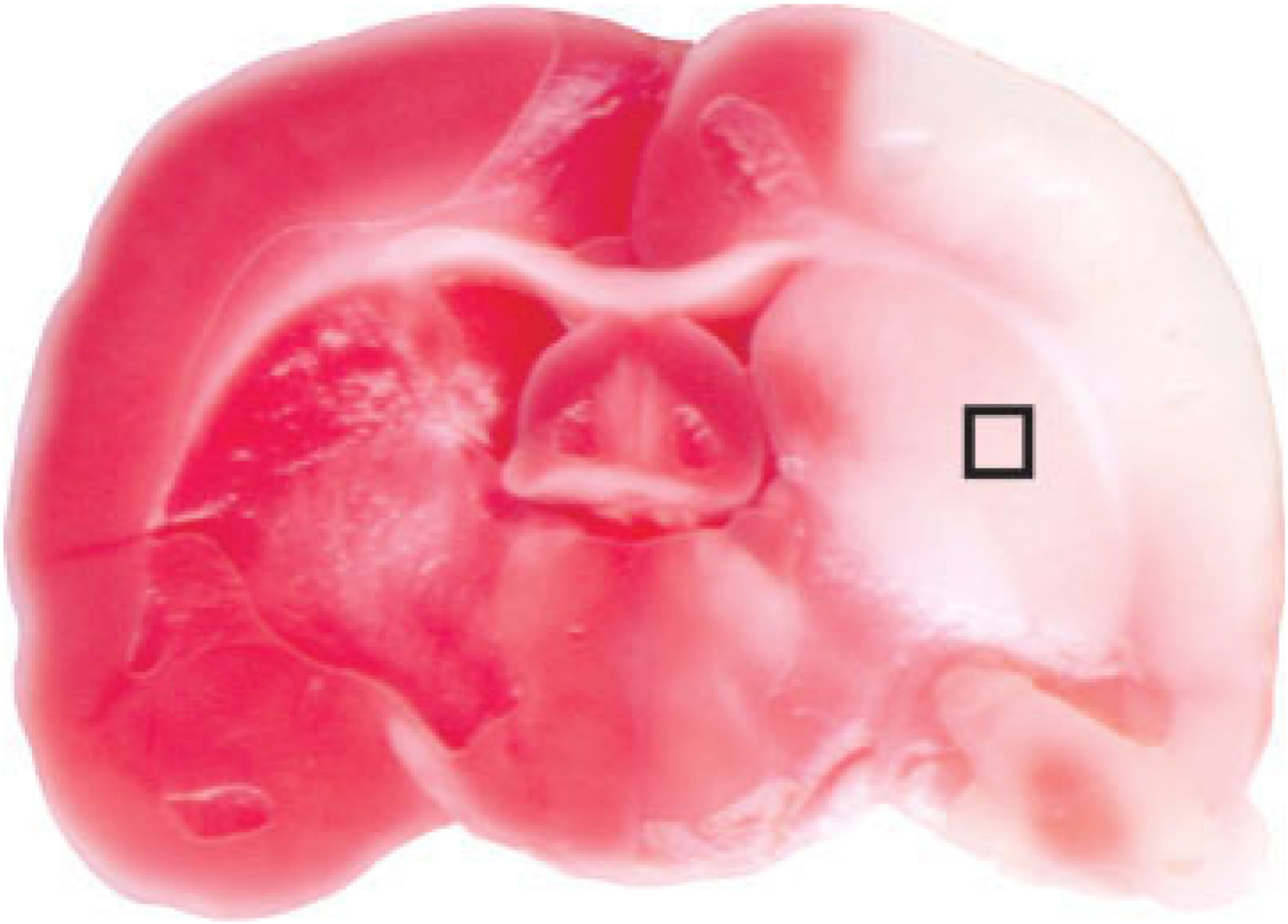

Fig. 1.
Representative image showing the area of infarction in a model used in this experiment (2% 2,3,5-triphenyltetrazolium chloride staining). The box indicates an area in the basal ganglia that was used for electron microscopic examinations.

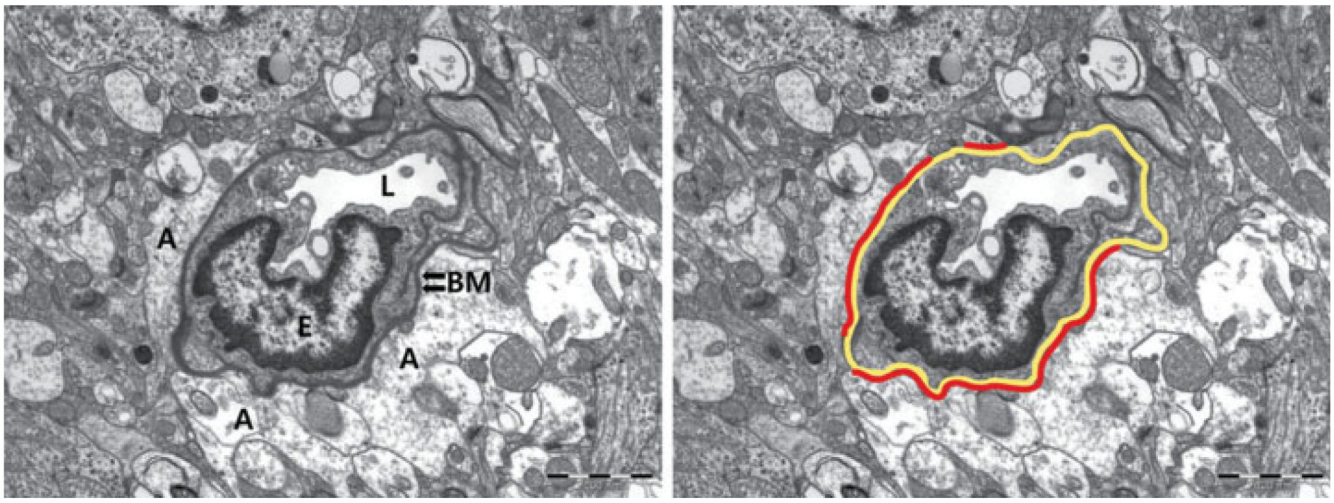

Fig. 2.

Measurement of the basement membrane and astrocyte endfeet contact. The percentage of the intact contact is calculated as [length of intact BM–astrocyte contact (red lines)/total circumferential length of the microvascular BM (yellow line) × 100]. A, astrocyte endfeet; BM, basement membrane; E, nucleus of an endothelial cell; L, lumen. Original magnification ×8,000.

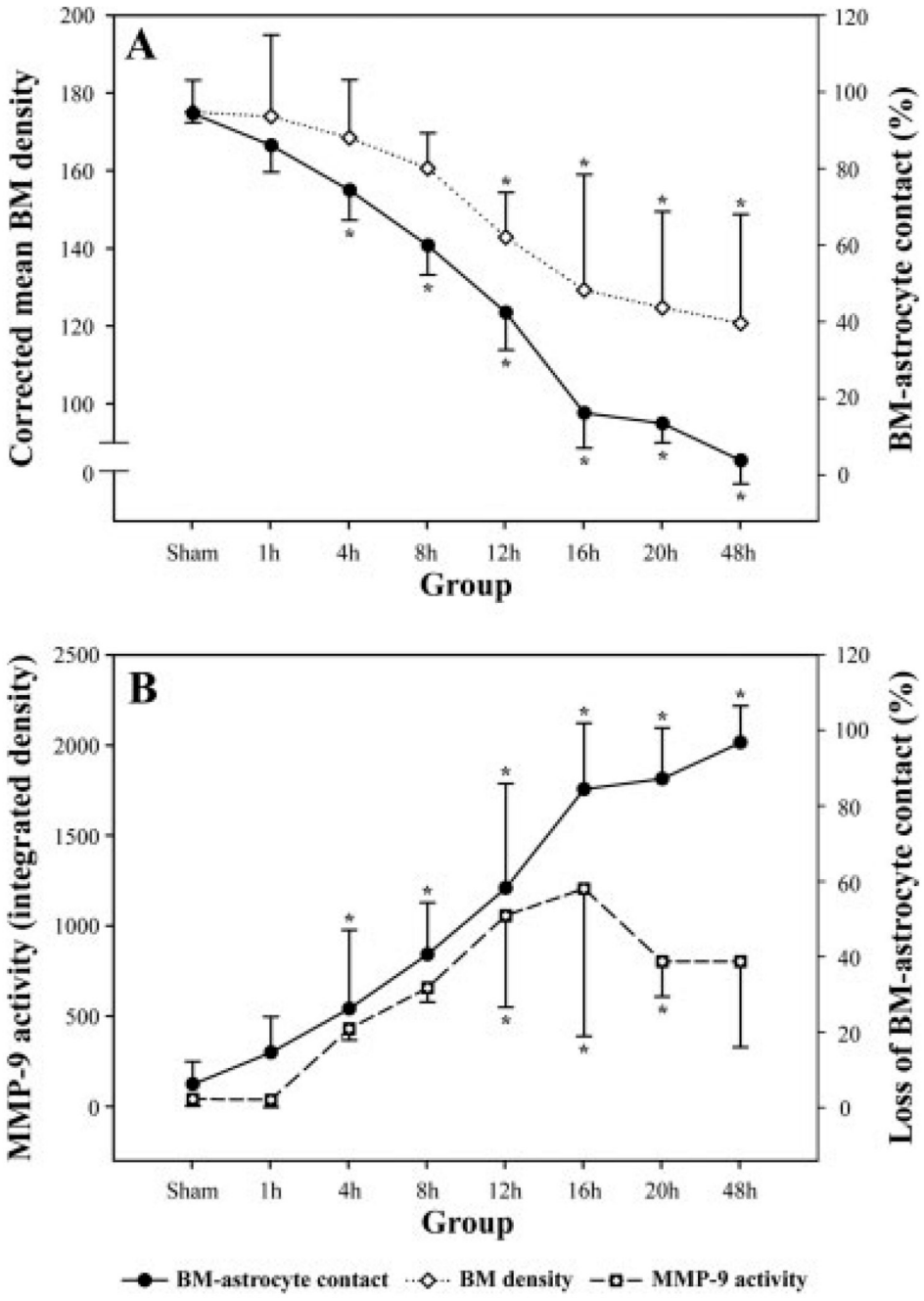

Fig. 3.

The temporal pattern of changes in the basement membrane (BM)–astrocyte contacts, BM electron densities, and MMP-9 activities at each time point after the middle cerebral artery occlusion (MCAO). Solid lines indicate the percentage of microvascular surface attached (**A**)/detached (**B**) to the enveloping astrocyte endfeet. The decrease is significant 4 hr after MCAO and thereafter compared with the sham-operated group. The BM density is significantly decreased at 12 hr and is further decreased until 48 hr. Changes in the BM–astrocyte contacts and BM densities appear parallel. The loss of contacts and the increase of MMP-9 activities also show a parallel pattern, particularly from 4 hr to 12 hr after MCAO. ★$P < 0.05$, significantly different from the sham.

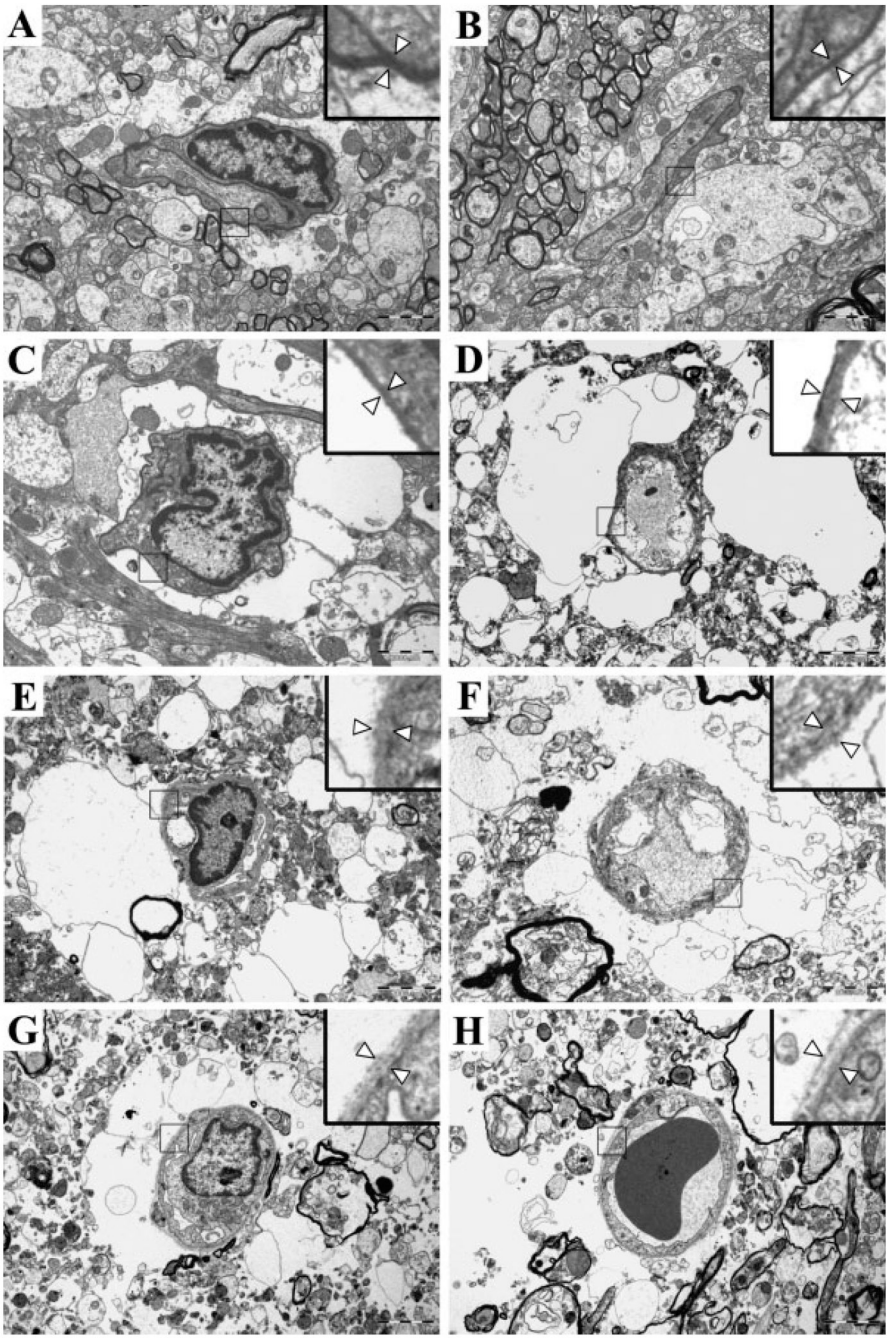

Fig. 4.

Representative electron microscopic photographs. **A:** Sham control. Almost all surface areas of the microvessel are covered by astrocyte endfeet. **B:** One hour after middle cerebral artery occlusion (MCAO). **C:** Four hours after MCAO. Swelling of the astrocytes and focal detachment of the astrocyte endfeet from the basement membrane (BM) are seen. **D:** Eight hours after MCAO. A marked astrocyte swelling and a further decrease in the intact portion of the contacts are demonstrated. **E:** Twelve hours after MCAO. The proportion of the intact BM–astrocyte contacts is markedly decreased, and the BM is damaged. **F:** Sixteen hours after MCAO. Further degradation of the BM and ruptured astrocytes is evident. **G:** Twenty hours after MCAO. There is excessive accumulation of water around the microvessels. **H:** Forty-

eight hours after MCAO. The astrocyte endfeet are no longer visible, and the BM is very faint. Arrowheads in the inset (magnified view) indicate the BM. Original magnification ×8,000.

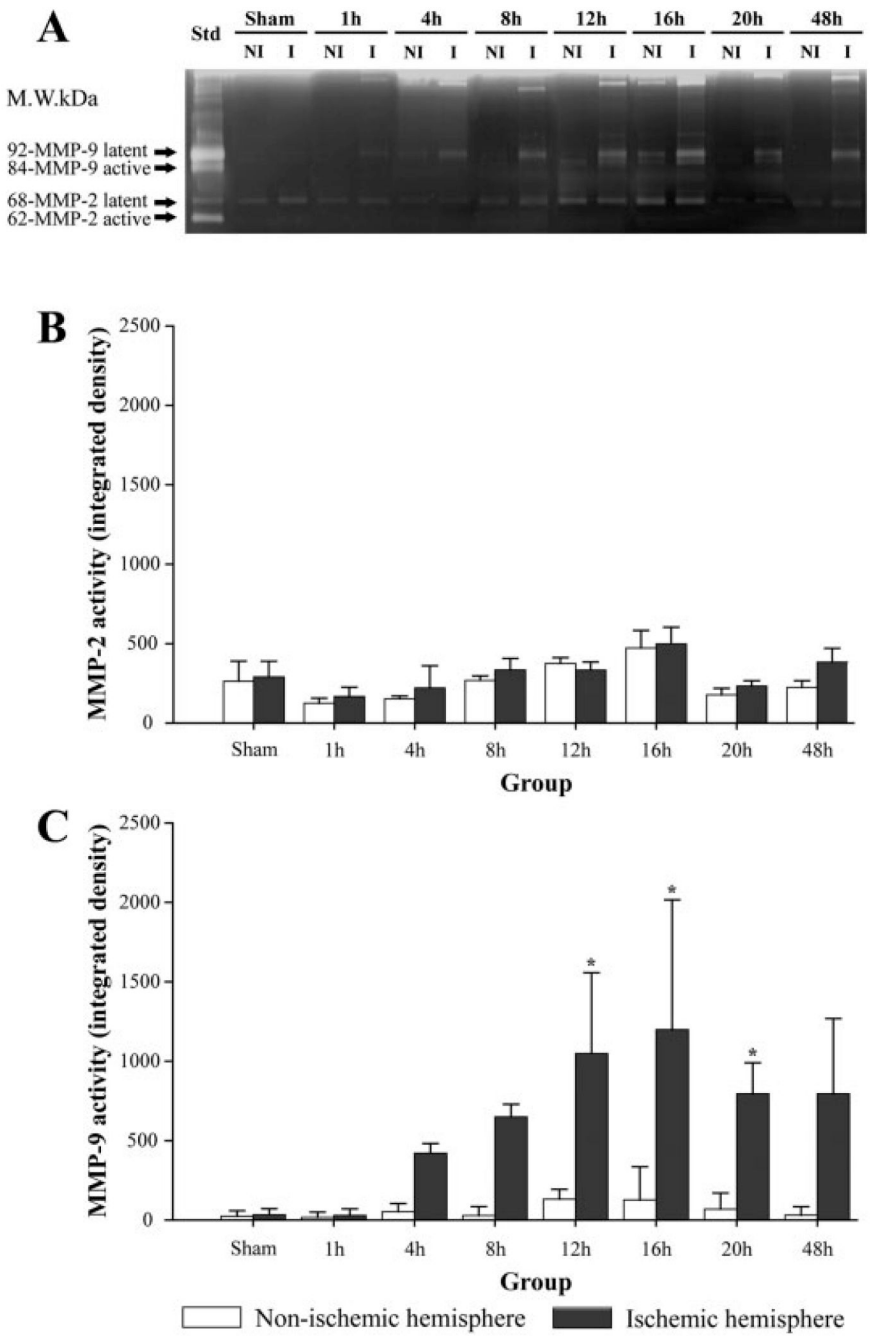

Fig. 5.

A: Representative zymograms showing clear bands of MMP-2 and MMP-9. **B:** There is no change in MMP-2 activities. **C:** MMP-9 activity is significantly increased at 12, 16, and 20 hr after middle cerebral artery occlusion (★$P < 0.05$). NI, nonischemic hemisphere; I, ischemic hemisphere; Std, mixture of recombinant MMP-2 and MMP-9 used as the standard.

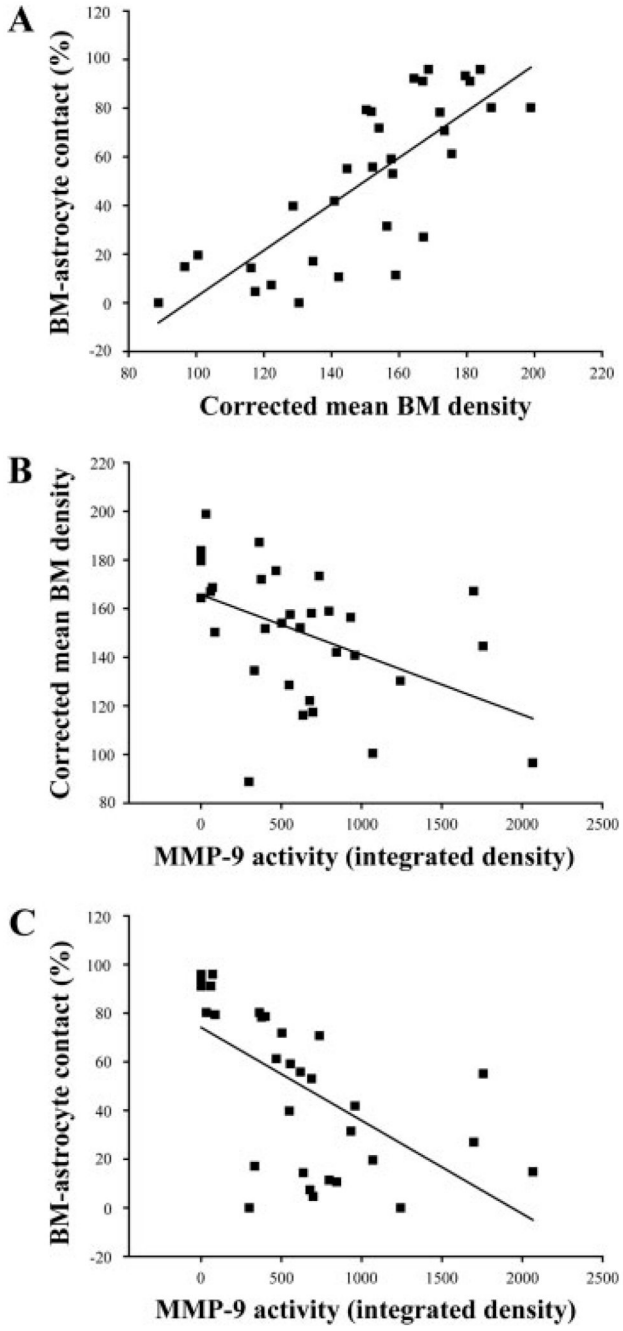

Fig. 6.

Correlations among percentages of the basement membrane (BM)–astrocyte contacts, mean electron densities of the BM, and MMP-9 activities. **A:** BM–astrocyte contacts and mean BM densities show a positive correlation (r = 0.784, $P < 0.001$). **B:** BM densities and MMP-9 activities show a negative correlation (r = −0.538, P 5 0.0016). **C:** BM–astrocyte contacts and MMP-9 activities show a negative correlation (r = −0.711, $P < 0.001$).